Korean J. Chem. Eng., 39(6), 1478-1486 (2022)
DOI: 10.1007/s11814-022-1064-9

pISSN: 0256-1115
eISSN: 1975-7220

Pyrolysis characteristics and quantitative kinetic model of microalgae *Tetralselmis* sp.

The Ky Vo*, Seung-Soo Kim,†, and Jinsoo Kim***,†**

*Department of Chemical Engineering, Industrial University of Ho Chi Minh City,
12 Nguyen Van Bao, Go Vap, Ho Chi Minh City, Vietnam
**Department of Chemical Engineering, Kangwon National University,
346 Joongang-ro, Samcheok, Gangwon-do 25913, Korea
***Department of Chemical Engineering (Integrated Engineering), Kyung Hee University,
1732 Deogyeong-daero, Yongin, Gyeonggi-do 17104, Korea
(*Received 25 November 2021 • Revised 28 December 2021 • Accepted 13 January 2022*)

Abstract−Pyrolysis of microalgal biomass is a potential strategy for biofuel production. In this work, the pyrolysis characteristics of microalgae, *Tetraselmis* sp., were systematically explored under isothermal and nonisothermal conditions. Analysis of nonisothermal decomposition of microalgae under nitrogen atmosphere at different heating rates (5, 10, 15, and 20 °C min^{-1}) revealed that the conversion of microalgae was significantly affected by the heating rate and reached ~90% at approximately 500 °C. The mean activation energy for the pyrolysis of *Tetraselmis* sp. was calculated using model-free Kissinger-Akahira-Sunose (KAS) and Flynn-Wall-Ozawa (FWO) methods. Microalgae pyrolysis in a micro-tubing reactor was performed at various temperatures (360-400 °C) and for different reaction times (0.5-3.0 min). The results indicated that the maximum yield of biocrude (49.5 wt%) was attained during pyrolysis at 400 °C for 2 min. It was established that the chemical composition of the biocrude was significantly influenced by the pyrolysis conditions. A quantitative model was used to evaluate the composition of carbohydrates, proteins, and lipids in the microalgae. This facilitated the determination of individual biochemical components in the pyrolytic products. Furthermore, the time- and temperature-dependent yields of the solid residue, biocrude, and gas were predicted, providing critical information for microalgal pyrolysis design, control, and performance.

Keywords: Pyrolysis, Microalgae, Biofuel, Tubing Reactor, Kinetic Model, Model Prediction

INTRODUCTION

Microalgae contain large amounts of biochemicals, such as carbohydrates, proteins, and lipids. This makes them versatile raw materials for producing renewable fuels (e.g., biodiesel, green diesel, bioethanol, methane, and fuel gases), value-added chemicals, and animal feed [1-4]. Moreover, the growth of microalgal biomass is significantly faster than that of lignocellulosic biomass. Thus, research concerning the conversion of microalgal biomass into biofuels has recently gained considerable attention [2-6].

Several strategies have been applied to convert biochemical components of microalgae into biofuels, including combustion, gasification, pyrolysis, and hydrothermal liquefaction [6,7]. Among the available approaches, pyrolysis has been generally utilized because it involves a single-step process, facilitating the efficient conversion of the majority of the biochemical constituents of raw biomass into helpful energy products [2,8-13]. Algal pyrolysis can produce biocrude, biochar, and biogas. Notably, microalgae-derived biocrude usually contains less oxygen and more hydrocarbons and exhibits a higher gross heating value than cellulosic biomass-derived biocrude [3]. Over the past few decades, numerous studies on the pyrolysis characteristics and products of microalgal pyrolysis have been conducted [2,5,14,15]. However, most of these investigations focused on the yield and quality of pyrolysis products. The lack of comprehensive understanding of the characteristics and kinetics of microalgal pyrolysis prevents the effective utilization of its potential on a large scale [3,4,16].

The pyrolytic behavior of microalgae has been predominantly explored by thermogravimetric analyses (TGA) in various environments. The TG method provides basic information about the decomposition of biochemical components upon the change in the pyrolysis temperature. The generated TG, and differential thermogravimetric (DTG) data can be combined with various mathematical models to estimate the apparent kinetic parameters (e.g., activation energy and preexponential factor) [3,17-22]. Nonetheless, the existing TGA methods can only provide weight loss and general information on the overall reaction kinetics rather than individual reactions, limiting their application [3]. Hence, TG/DTG experiments cannot be used to acquire information, which would result in high yields and good quality pyrolytic products.

Many attempts have been made to develop models for microalgal pyrolysis. For example, Vo et al. [7] proposed a lumped kinetic model for the pyrolysis of microalgae in a micro-tubing reactor, which could be used to determine the kinetic parameters of different reaction pathways (i.e., biomass→bio-oil, biomass→gas, and bio-oil→gas). Furthermore, Bach et al. [23] studied the pyrolysis

†To whom correspondence should be addressed.
E-mail: sskim2008@kangwon.ac.kr, jkim21@khu.ac.kr

characteristics of microalgae, *Chlorella vulgaris* sp., employing a TG/DTG method. They constructed several reaction models, which enabled the establishment of kinetic parameters for individual thermal decomposition of carbohydrates, lipids, and proteins. However, the proposed models did not reveal the contribution of individual biochemical components of the microalgae to the generated solid residue, bio-oil, and gas. More recently, Hong et al. [24] performed a pyrolysis kinetic study of three primary components of lipids, carbohydrates, and proteins, as well as microalgae *Spirulina*, using TGA under N_2 and CO_2 atmosphere. Although the above studies describe the pyrolysis behavior of microalgal biomass, the development of a model that can quantitatively evaluate the contributions of each biochemical component to the pyrolytic products with regards to experimental conditions (e.g., temperature and time) is required. It would provide crucial information for designing and applying large-scale microalgal pyrolysis processes. In addition, a comprehensive understanding of the effects of the biochemical composition of microalgae on the yield and quality of pyrolytic products would enable the classification and planning of the potential microalgal feedstock.

This work investigates the pyrolysis characteristics of microalgal *Tetraselmis* sp. by TGA analyses and pyrolysis in a micro-tubing reactor. The TGA data obtained at various heating rates were combined with model-free methods to estimate the activation energy for the conversion of microalgal biomass. Microalgae conversion in a micro-tubing reactor was conducted at various pyrolysis temperatures (360-400 °C) and time (0.5-3 min). It was observed that the pyrolytic product distribution and the composition of biocrude were strongly influenced by the pyrolysis conditions. The acquired data was subsequently utilized to design a quantitative model, which facilitated the determination of the contribution of individual reactions of carbohydrates, proteins, and lipids in microalgae cells to biocrude and gaseous products. The reaction rate constant and activation energy for each reaction pathway was established through an optimization function (MATLAB) to evaluate the contribution of each biochemical component. Moreover, a prediction model was then constructed based on the resulting kinetic parameters to predict the yields of solid residues, bio-oil, and gas as a function of pyrolysis temperature and time.

EXPERIMENTAL METHODS

1. Materials

The *Tetraselmis* sp. biomass was cultured in seawater for 18 days using a photobioreactor [6,25]. The cells were harvested by centrifugation and preserved by freeze-drying. The ash content of the microalgal biomass was determined by ASTM E1755. Elemental analysis involved using an elemental analyzer (Flash EA1112, Thermo Finnigan, CA, USA). Analyses of the functional groups of the microalgae employed Fourier-transform infrared spectroscopy (FT-IR) (Perkin-Elmer, Buckinghamshire, UK). The obtained results revealed the vibration modes of different organic functional groups, including N-H and O-H (3,440-3,680 cm^{-1}), C=O of amide I (1,642 cm^{-1}), and C-O (1,400-1,500 cm^{-1}) [26,27] (Fig. 1). Using previously reported procedures, the content of carbohydrates, lipids, and proteins in *Tetraselmis* sp. was determined to be 29.30 wt%, 26.12 wt%, and 38.46 wt%, respectively (Table 1) [6,7].

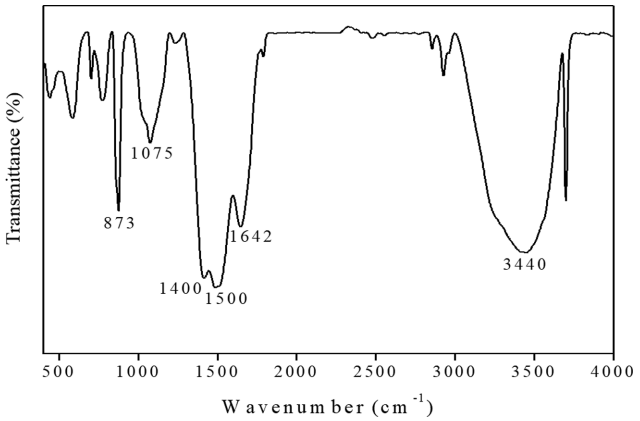

Fig. 1. Fourier-transform infrared spectrum of microalgae *Tetraselmis* sp.

Table 1. Ultimate and proximate analyses of microalgae *Tetraselmis* sp.

Component	Composition
Ultimate analysis (wt%, dry ash free)	
C	40.23
H	9.03
O	6.89
N	43.85
Proximate analysis (wt%, dry basis)	
Carbohydrates	29.30
Lipids	26.12
Proteins	38.46
Ash	6.12

2. Thermogravimetric Analysis

TGA of microalgae *Tetreaselmis* sp. was performed using a TGA analyzer (Q50, TA Instruments, New Castle, USA). The nonisothermal pyrolysis was conducted at temperatures varying from room temperature to 700 °C with 5, 10, 15, and 20 °C/min heating rates under a nitrogen atmosphere. For each run, 10±1.0 mg of dried microalgal biomass was loaded, and the weight loss was measured as a function of temperature.

3. Pyrolysis of Microalgae in a Micro-tubing Reactor

Fig. 2 shows a schematic of the pyrolysis of microalgae, *Tetraselmis* sp., employing a micro-tubing reactor (volume: 8 mL). A molten salt bath containing a eutectic salt of KNO_3 (59 wt%) and $Ca(NO_3)_2$ (41 wt%) was used to heat the reactor [6,7,28]. 1.5±0.20 g of microalgae, *Tetraselmis* sp., was loaded into the micro-pyrolyzer for each run. Subsequently, the reactor was placed into the molten salt bath, set up at a specified temperature of 360 °C, 380 °C, or 400 °C. After a specific reaction time, the reactor was immediately quenched in an ice-water bath to cool for one h. The reactor was then opened to release the gaseous products. The produced mixture, containing a biocrude and solid residue, was collected and washed with acetone (Sigma Aldrich, 98%) to obtain an acetone-insoluble solid residue and an acetone-soluble biocrude. The weight of the gas

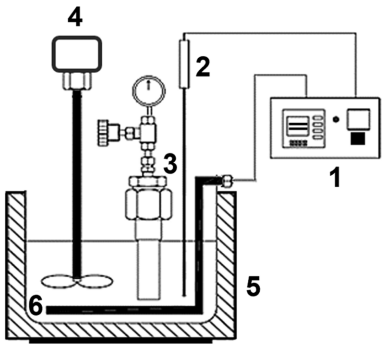

Fig. 2. Schematic of the pyrolysis of microalgae in a micro-tubing reactor.

1. PID temperature controller
2. Thermocouple
3. Tubing reactor
4. Stirrer
5. Salt bath
6. Heater

product was obtained by weighing the reactor before and after releasing the gas. The yield of the product was calculated based on the dry basis of the loaded sample. The moisture content in the produced biocrude fraction was determined using Karl Fischer titration. The chemical composition of the biocrude was analyzed by gas chromatography-mass spectrometry (GC-MS) (Agilent 7890A, Agilent Technologies, USA) using an HP-5MS capillary column.

RESULTS AND DISCUSSION

1. Thermogravimetric Analysis

Nonisothermal TGA of *Tetralselmis* sp. was conducted at different heating rates of 5, 10, 15, and 20 °C min^{-1}. Fig. 3(a) and 3(b), 3(c) show the TGA and DTG curves of the biomass sample at the different heating rates, respectively. It was found that higher heating rates accelerated the conversion of the microalgae. The DTG curves revealed that the values of T_{max}, corresponding to the temperature at which the maximum rate of weight loss is observed, increased from 317 °C to 345 °C, 353 °C, and 376 °C with increasing heating rate from 5 °C min^{-1} to 10, 15, and 20 °C min^{-1}, respectively [Fig. 3(b)]. Notably, most of the microalgal biomass was decomposed in the temperature range of 200-600 °C, resulting in a major weight loss of ~90%. The DTG curve acquired at a heating rate of 10 °C min^{-1} was deconvoluted to gain inside the thermal decomposition behavior of individual biochemical components [Fig. 3(c)]. As can be seen, the deconvoluted DTG curve exhibited three large peaks, which were attributed to the thermal decomposition of carbohydrates (262 °C), proteins (346 °C), and lipids (432 °C), respectively. Similar thermal degradation behavior was observed for other microalgae, such as *Nannochloropsis oculata* [1], *Chlorella vulgaris* sp. [23], *Chlorella sorokiniana* [29], and *Aurantiochytrium* sp. [17].

Furthermore, the activation energy for the pyrolysis of microalgae *Tetraselmis* sp. was estimated by combining TGA and model-free methods. We employed two widely applied model-free methods, namely Kissinger-Akahira-Sunose (KAS) [17,30] and Flynn-Wall-Ozawa (FWO) [18,31], which could be expressed by Eq. (1) and Eq. (2), respectively:

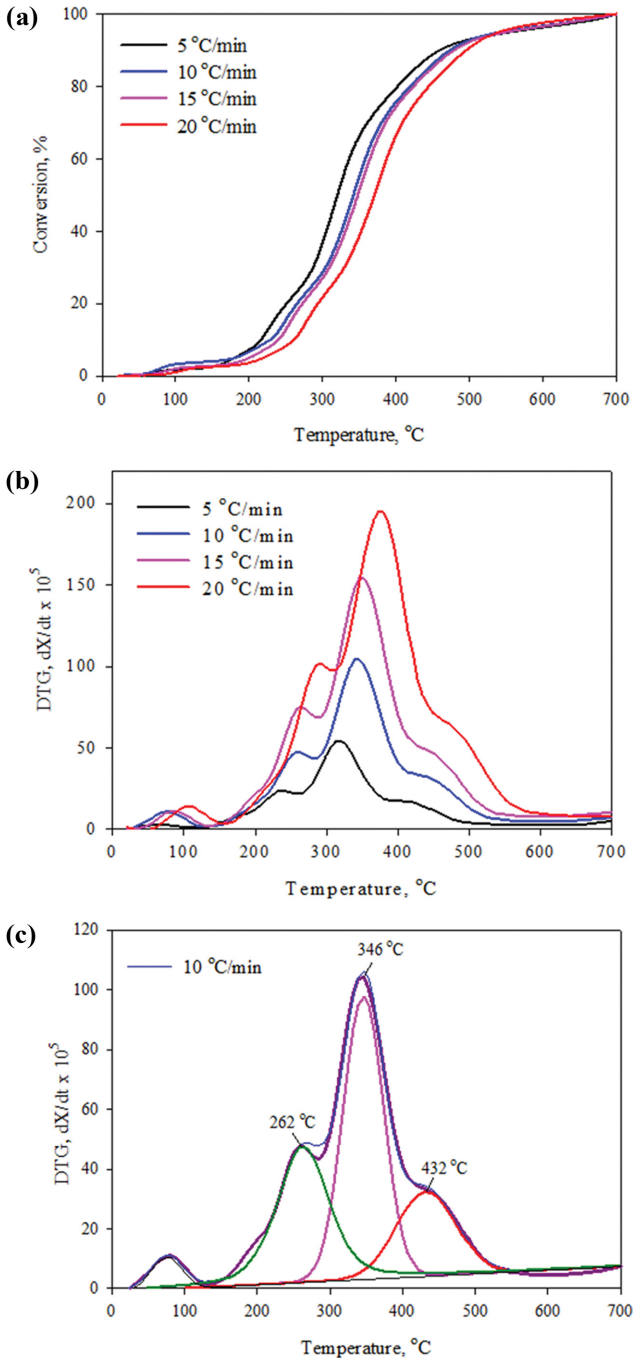

Fig. 3. Thermogravimetric analyses (TGA) of *Tetraselmis* sp.: (a) TGA curves at different heating rates, (b) differential thermogravimetric (DTG) curves at different heating rates, and (c) deconvoluted DTG curve obtained at a heating rate of 10 °C min^{-1}.

$$\ln\left(\frac{\beta}{T^2}\right)=\ln\left[\frac{AR}{Eg(X)}\right]-\frac{E}{RT} \quad (1)$$

$$\ln(\beta)=\ln\left(\frac{AE}{Rg(X)}\right)-5.331-1.052\frac{E}{RT} \quad (2)$$

where, X, A, and E refer to the conversion of biomass (%), preexponential factor, and apparent activation energy (kJ mol^{-1}), respec-

tively. R, T, and β indicate the universal gas constant, absolute temperature (K), and heating rate (K min^{-1}), respectively.

The plots for the KAS and FWO methods are presented in Fig. 4, and the calculated activation energy values with respect to the conversion are summarized in Table 2. It can be seen that the values obtained using these methods are relatively similar. As presented in Table 2, the apparent activation energy increased with increasing the conversion of the microalgae. The increase of the conversion from 10% to 60% was predominantly caused by the decomposition of carbohydrates and proteins in the cells. According to the KAS method, at this stage, the activation energy gradually increased from 109.65 to 156.15 kJ mol^{-1}. However, the activation energy rapidly increased from 156.15 to 196.32 kJ mol^{-1} when the conversion increased from 60% to 90%. This was primarily caused by the thermal decomposition of lipids in the cells, indicating that a higher energy input was required to decompose lipids in the microalgal cells. Based on the KAS and FWO methods, the values of the average activation energy for the thermal conversion of *Tetraselmis* sp. were approximately 150.06 and 148.83 kJ mol^{-1}, respectively. These values were marginally lower than that previously reported for *Tetraselmis* sp. (~170 kJ mol^{-1}) [1]. This difference might be attributed to the different biochemical compositions, which resulted from varying cultivation conditions [4,6].

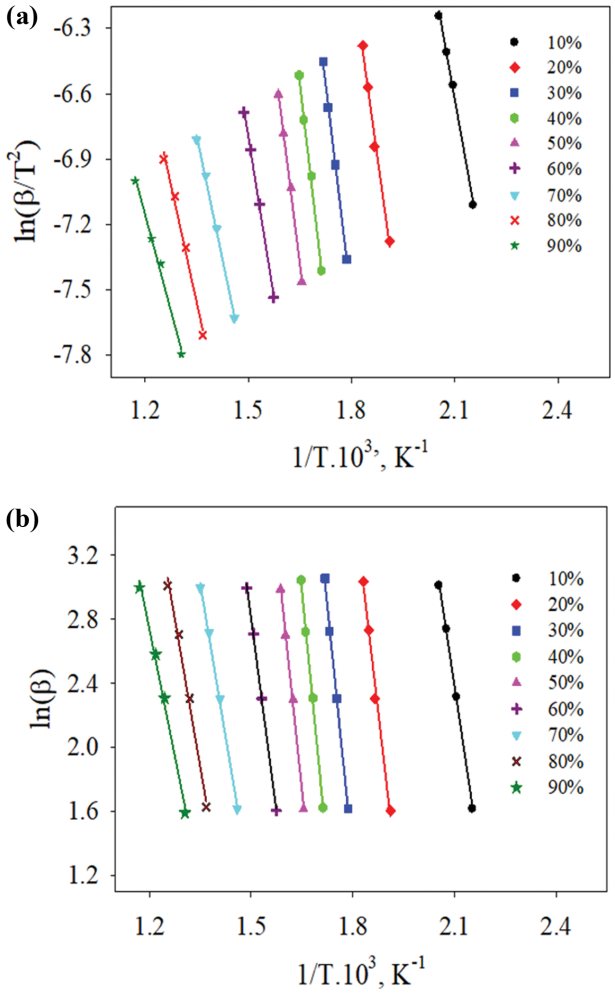

Fig. 4. Model plots for the pyrolysis of *Tetraselmis* sp. at different conversions using (a) KAS and (b) FWO methods.

Table 2. Activation energy obtained using the KAS and FWO methods

Conversion, %	KAS		FWO	
	E_a, kJ mol^{-1}	R^2	E_a, kJ mol^{-1}	R^2
10	109.65	0.987	106.79	0.988
20	117.26	0.979	114.91	0.978
30	129.13	0.988	128.45	0.999
40	137.35	0.999	135.80	0.998
50	144.76	0.997	145.23	0.996
60	156.15	0.998	153.87	0.996
70	179.46	0.996	177.12	0.997
80	184.65	0.995	182.62	0.995
90	196.32	0.994	194.67	0.995
Average	***150.06***		***148.83***	

2. Distribution of Pyrolysis Products and Analysis of Bio-oil

According to the data obtained from TGA, most of the biomass of *Tetraselmis* sp. decomposed in the temperature range of 360-400 °C. Hence, the pyrolysis in a micro-tubing reactor was performed at three temperatures: 360 °C, 380 °C, and 400 °C. Table 3 shows the distribution of pyrolytic products, including bio-oil, gaseous products, and solid residue. As shown, the conversion of microalgae increased with increasing pyrolysis temperature and holding time. Under the employed pyrolysis conditions, the products consisted of 31.75-84.60 wt% of solid residue, 14.7-49.5 wt% of bio-oil (biocrude), and 1.20-14.10 wt% of gas. The water content of the bio-oil obtained at 380 °C and 400 °C, analyzed by Karl Fisher titration, was 1.12 and 1.65 wt%, respectively. At 360 °C and 380 °C, the yield of bio-oil increased with increasing holding time. The maximum yield of bio-oil (~49.5 wt%) was obtained at 400 °C

Table 3. Biocrude, gas, and solid residue produced from the pyrolysis of *Tetraselmis* sp. in a micro-tubing reactor

Pyrolysis conditions	Biocrude, wt%	Gas, wt%	Solid, wt%
360 °C			
0.5 min	14.70±3.55	1.20±0.45	84.13±2.51
1 min	15.89±4.21	4.31±1.27	79.80±4.56
2 min	30.38±5.10	5.42±2.38	64.20±3.49
3 min	36.43±3.78	8.10±3.43	55.47±3.09
380 °C			
0.5 min	15.32±3.87	2.45±1.08	82.23±2.30
1 min	24.17±6.12	4.65±1.61	71.18±2.15
2 min	33.41±7.34	6.19±2.13	60.40±3.07
3 min	45.36±5.58	9.73±3.80	44.91±2.34
400 °C			
0.5 min	17.34±3.24	3.20±1.23	72.56±3.20
1 min	34.79±3.67	5.50±1.60	52.81±4.11
2 min	49.48±5.82	7.45±2.34	35.99±3.25
3 min	48.27±6.15	16.56±2.78	28.34±2.87

Table 4. Gas chromatography-mass spectrometry analysis of biocrude produced at 380 °C and 400 °C in a micro-tubing reactor

No.	Residence time, min	Compounds	Peak area, %		Structure
			380 °C	400 °C	
1	4.140	2-Hexanone	1.4	1.1	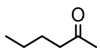
2	6.140	2-Pentanone, 4-amino-4-methyl-	2.51	-	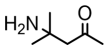
3	9.400	Pentanal, 2,2-dimethyl-	-	3.68	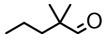
4	10.740	Phenol	1.39	2.89	
5	11.331	Butanamide, 3-methyl-	1.01	1.04	
6	13.386	Methyl (1-acetyl-2-piperidinyl)(phenyl)acetate	4.61	1.1	
7	13.726	2-Pyrrolidinone	5.1	2.1	
8	13.950	Phenol, 4-methyl-	1.81	4.95	
9	14.950	2,2,6,6-Tetramethyl-4-piperidone	7.65	8.91	
10	15.600	Benzyl nitrile	1.01	1.24	
11	15.970	2,5-Pyrrolidinedione	6.46	1.5	
12	17.183	3-Pyridinol, 6-methyl-	4.08	1.07	
13	17.740	Dianhydromannitol	2.00	2.10	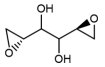
14	18.650	Benzenepropanenitrile	-	1.55	
15	20.200	Indole	-	2.2	
16	30.170	Psoralene	-	2.01	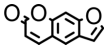
17	34.230	Hexadecanenitrile	3.40	1.51	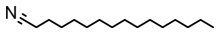
18	34.780	Hexadecanoic acid, methyl ester	2.61	3.81	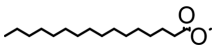
19	35.227	1,4-diaza-2,5-dioxo-3-isobutyl bicyclo[4.3.0]nonane	2.23	-	
20	35.800	Hexadecanoic acid	1.5	6.25	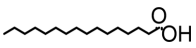
21	38.060	9-Octadecenoic acid, methyl ester, (E)-	1.02	8.52	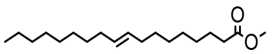
22	38.510	Octadecanoic acid, methyl ester	-	1.18	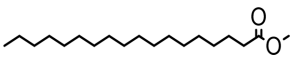
23	38.950	9-Octadecenoic acid (Z)-	-	7.42	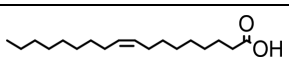
24	39.540	Hexadecanamide	-	1.17	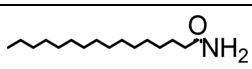
25	48.070	Tetracosanoic acid, methyl ester	-	1.2	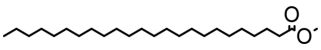
26	53.390	Octacosanoic acid, methyl ester	-	2.02	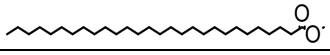
		Total (%)	**49.79**	**70.34**	

with a holding time of 2 min. In the literature, bio-oil yield is in the range of 24-43 wt% at a pyrolysis temperature of 500 °C [32,33]. Note that the bio-oil yield strongly depends on the biomass's biochemical composition and pyrolysis condition such as temperature, time, and reactor type. The findings in this work suggest that microalgal *Tetraselmis* sp. can produce a high biocrude yield via fast pyrolysis conditions of 380 °C within 2 min. However, further increasing the reaction time to 3 min at the same temperature resulted in a slight decrease in bio-oil yield. This could be due to the partial decomposition of biocrude to a gas product at high temperatures [17,31]. These findings suggest that the pyrolysis conditions of 400 °C and holding time of 2 min were optimal for converting microalgae *Tetraselmis* sp. To further investigate the effects of the pyrolysis conditions, the biocrude products produced at 380 °C and 400 °C were analyzed by GC-MS, and their chemical composition was compared. Table 4 shows the chemical composition of the produced bio-oil fractions as determined using GC-MS (only compounds with a match quality of at least 90%). It was found that the biocrude obtained at 400 °C contained more chemical components than that produced at 380 °C. This could be explained by the acceleration of the decomposition of macro-biochemicals in the microalgae at higher temperatures. In addition, the biocrude produced at the pyrolysis temperature of 380 °C was predominantly composed of nitrogen-containing compounds (~33.46%), which were generated from the decomposition of proteins. In contrast, the biocrude generated at 400 °C contained a significant amount of fatty acids and esters (~30.4%), which were probably produced due to lipid decomposition. This is in good agreement with the TGA, which indicates that the lipids in microalgae were more thermally stable than proteins. This finding suggests that lipids and proteins are the major contributors to the pyrolytic biocrude fraction. Previous studies also found that the contribution of individual components into microalgae-derived biocrude follows the order: lipids> proteins>carbohydrates [15,34].

3. Kinetic Model for Pyrolysis of Microalgae *Tetraselmis* sp.

The classification and evaluation of microalgal biomass resources based on their biochemical composition are critical. Thus, we subsequently considered the distribution of each biochemical component in every pyrolytic fraction. The time- and temperature-dependent yields of the solid residue, biocrude, and gas, obtained from the decomposition of microalgae in a micro-tubing reactor, were utilized to develop a quantitative kinetic model. In the model, carbohydrates, proteins, and lipids in the cells were supposed to decompose to biocrude and gas products individually. During the pyrolysis process, the produced biocrude was also converted to gas (Fig. 5).

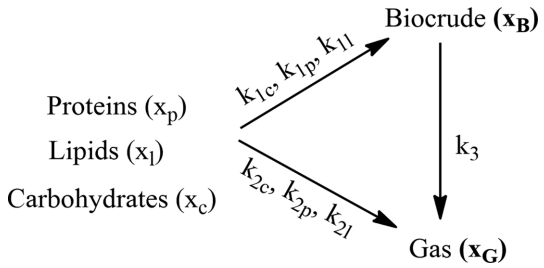

Fig. 5. Reaction network for the pyrolysis of *Tetraselmis* sp. in a micro-tubing reactor.

All reaction pathways were assumed to be irreversible and follow first-order kinetics. Accordingly, the apparent rate equations could be expressed as follows:

$$\text{Carbohydrates: } -\frac{dx_c}{dt} = (k_{1,c} + k_{2,c})x_c \quad (3)$$

$$\text{Proteins: } -\frac{dx_p}{dt} = (k_{1,p} + k_{2,p})x_p \quad (4)$$

$$\text{Lipids: } -\frac{dx_l}{dt} = (k_{1,l} + k_{2,l})x_l \quad (5)$$

$$\text{Bio-oil: } -\frac{dx_B}{dt} = k_{1,c}x_c + k_{1,p}x_p + k_{1,l}x_l - k_3x_B \quad (6)$$

$$\text{Gas: } -\frac{dx_G}{dt} = k_{2,c}x_c + k_{2,p}x_p + k_{2,l}x_l + k_3x_B \quad (7)$$

where, x_c, x_p, x_l, x_B, and x_G indicate the mass fractions of carbohydrates, proteins, lipids, biocrude, and gas product, respectively, whereas k_{ij} refers to the reaction rate constants. The mass fraction of each biochemical component was calculated based on the ash-free biomass (x), which was expressed as follows:

$$x = x_c + x_p + x_l \quad (8)$$

We simultaneously solved the system of ordinary differential Eqs. (3)-(8) and estimated values for the rate constants (k_{ij}) using a least-squares objective function [Eq. (9)]:

$$P = \sum_i \sum_t (x_i^{experimental} - x_i^{model})^2 \quad (9)$$

The residual, shown in Eq. (9), is the summation of the squared differences, at a given liquefaction temperature, between the experimental yield for each product fraction ($x_i^{experimental}$) and the model value (x_i^{model}). Herein, we used the MATLAB optimization function, 'fmincon', selecting the 'interior-point' algorithm to minimize the value of the residual at each temperature [7,31,35,36]. The boundary conditions for the values of k_{ij} in the range of 0.0-0.48 min^{-1}. The upper bound was constrained at 0.48 min^{-1} since this value was large enough to accommodate the fastest paths observed experimentally but small enough to avoid longer computational times. The optimized values of the rate constants for each reaction pathway at each temperature are included in the supplemental information.

Figs. 6(a)-(c) compare the calculated models (solid lines) with the experimental data (discrete points) at different temperatures. The results reveal that the model captured the experimental results well. At low pyrolysis temperatures of 360 °C and 380 °C, the yield of pyrolyzed biocrude gradually increased with increasing temperature, attaining conversions of ~37% and ~52%, respectively. At 400 °C, >70% of the microalgal biomass was decomposed within 3 min. At this temperature, the yield of bio-oil reached the maximum value within 2 min. Subsequently, the yield marginally decreased with increasing holding time. In contrast, the gas yield gradually increased with increasing reaction temperature and time.

Table 5 summarizes the obtained values of k_{ij} and activation

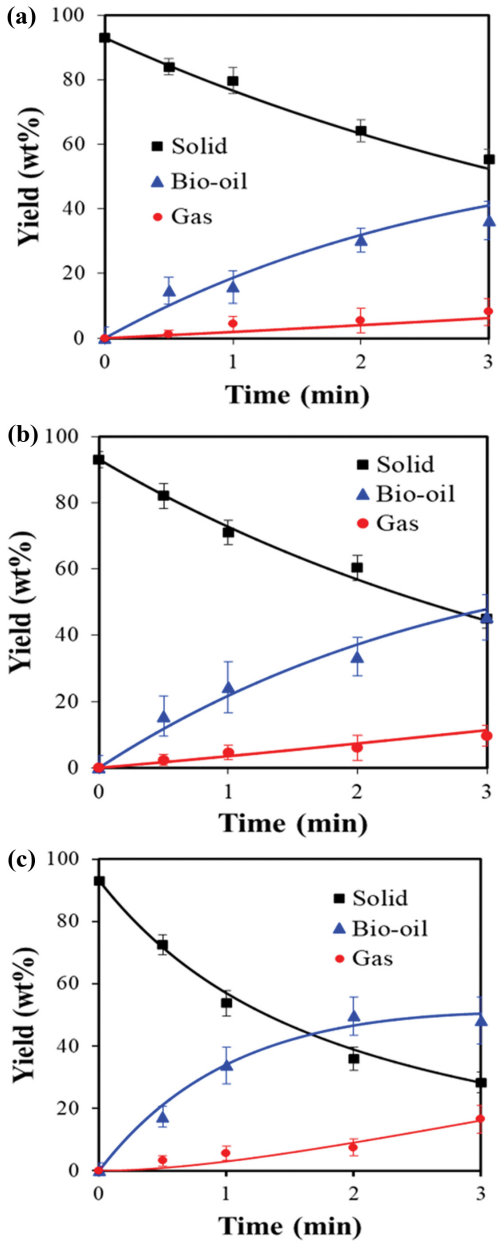

Fig. 6. Experimental (discrete points) and calculated (dash lines) yields of solid, bio-oil, and gas as a function of reaction time at various temperatures: (a) 360 °C, (b) 380 °C, and (c) 400 °C.

energy for all the reactions. As shown, the rate constants for the reactions of the biochemical components to biocrude are significantly larger than those for the conversion of biochemical components to the gas phase. This indicates that carbohydrates, proteins, and lipids were the main contributors to the biocrude phase. At low temperatures, the conversion of carbohydrates into biocrude exhibited the highest reaction rate constant. However, at a higher temperature of 400 °C, the reaction rate constant for the decomposition of proteins exceeded that for the decomposition of carbohydrates and lipids. The results evidence that the breakage of the protein structure is considerably accelerated at high temperatures. As shown in Table 5, the pathway from biocrude to gas is more favorable than microalgal biomass to gas. This is attributed to the smaller structures of biocrude, which are more easily thermally decomposed. The mean values of the activation energy for each reaction pathway are shown in Table 5. It was determined that the activation energy values for converting carbohydrates, proteins, and lipids in the microalgae cells to bio-oil were ~108, 133, and 152 kJ mol^{-1}, respectively. In addition, the activation energy for the production of gas from carbohydrates, proteins, and lipids was 237, 221, and 254 kJ mol^{-1}, respectively. It can be seen that the conversion of bio-oil to gas required the lowest activation energy of ~103 kJ mol^{-1}. Bach et al. [23] reported the activation energy for the conversion of carbohydrates (74-222 kJ mol^{-1}), proteins (207-221 kJ mol^{-1}), and lipids (~113 kJ mol^{-1}), which were calculated based on the nonisothermal pyrolysis of microalgae *Chlorella vulgraris* sp. Moreover, Hong et al. [24] found that the activation energy for the pyrolysis of algae's carbohydrates, proteins, and lipids was ~227.8, 74.4, and 121.7 kJ mol^{-1}, respectively. Generally, the energy for the conversion of each primary component of algae varies due to their different chemical compositions and the effect of the pyrolysis conditions [24].

Model prediction of the product distribution can provide essential information for the effective design and control of the pyrolysis process. In the present work, the proposed model predicted the product distributions over a wide range of temperatures (340-420 °C) and reaction time (0-6 min). Fig. 7(a) shows the predicted distribution of the solid residue, suggesting that at 420 °C, more than 80% of the microalgae decomposed within the first 2 min. Most of the microalgae were decomposed upon a further increase in the holding time up to 6 min. The predicted distribution of the bio-oil yield is demonstrated in Fig. 7(b). At a low temperature of

Table 5. Reaction rate constant and activation energy for individual reaction pathways

Reaction pathway	k_j, wt% min^{-1}			E_j, $kJmol^{-1}$	lnA
	360 °C	380 °C	400 °C		
Carbohydrates→Biocrude	0.1220	0.2880	0.414	108±10	20.84
Proteins→Biocrude	0.1040	0.2760	0.476	133±15	23.39
Lipids→Biocrude	0.0628	0.1194	0.352	152±19	18.55
Carbohydrates→Gas	0.0016	0.0198	0.023	237±27	39.01
Proteins→Gas	0.0034	0.0278	0.041	221±22	36.47
Lipids→Gas	0.0014	0.0097	0.022	254±28	43.14
Biocrude→Gas	0.0780	0.1380	0.252	103±8	17.16

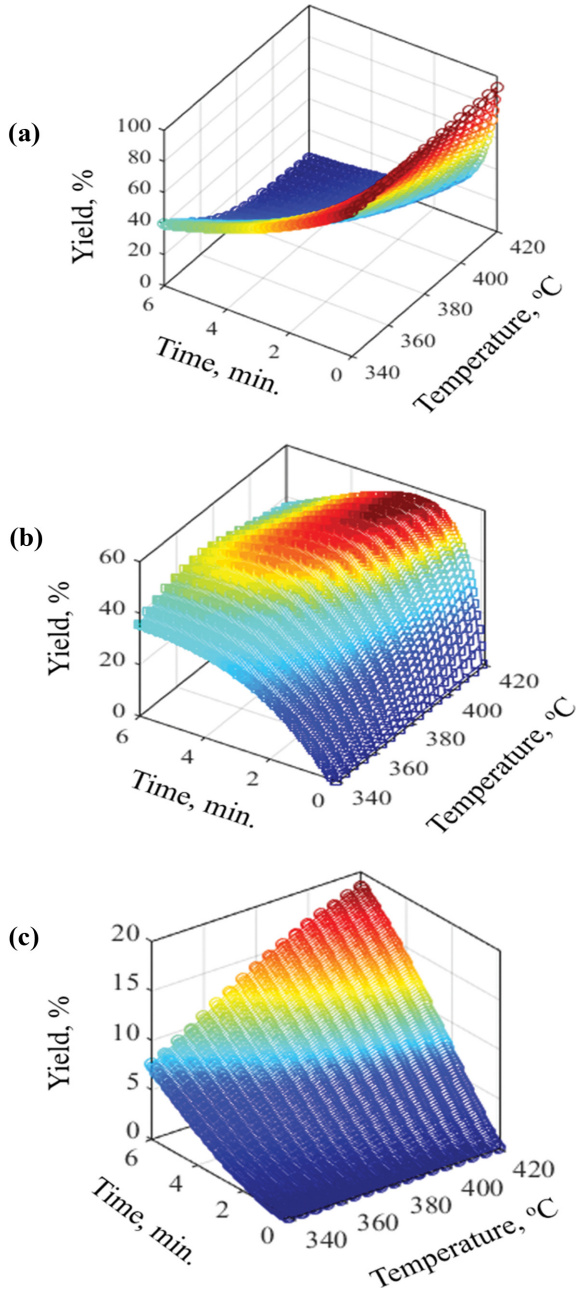

Fig. 7. Model prediction of the yields of (a) solid residue, (b) biocrude, and (c) gas as a function of the reaction time and temperature.

340 °C, the yield of biocrude steadily increased with increasing holding time, reaching approximately 40 wt% after 6 min. However, at a higher pyrolysis temperature of 420 °C, the yield of the biocrude rapidly increased within the first few minutes and then diminished with longer pyrolysis time. The maximum biocrude yield of ~56 wt% was predicted under pyrolysis conditions of 420 °C and 1.5 min. The predicted distribution of gas yield [Fig. 7(c)] suggested that the gas yield increased with increasing reaction temperature and holding time. A low temperature of 340 °C resulted in a gradual increase in the gas yield with increasing time. Nevertheless, at 420 °C, the gas evolution increased with increasing pyrolysis time, and the yield was predicted at ~19 wt% after 6 min.

CONCLUSIONS

The pyrolysis of microalgae *Tetraselmis* sp. was systematically investigated under nonisothermal and isothermal decomposition conditions. Under nonisothermal conditions, the decomposition of microalgae was accelerated at a higher heating rate, showing a significant weight loss (~90%) at 500 °C due to the decomposition of carbohydrates, proteins, and lipids in the microalgae cells. Using the KAS and FWO methods, the average activation energy corresponding to the conversion in the range of 10-90% was determined to be approximately 150.06 and 148.83 kJ mol^{-1}, respectively. *Tetraselmis* sp. was effectively decomposed in a micro-tubing reactor, producing a maximum biocrude yield of ~49.5% within a short reaction time of 2 min. At a low pyrolysis temperature (<380 °C), the obtained biocrude contained a considerable amount of N-containing compounds generated from the decomposition of proteins in the cells. Moreover, a higher temperature (400 °C) accelerated the decomposition of lipids in the microalgal biomass. The proposed quantitative model, which consisted of individual conversions of carbohydrates, proteins, and lipids into pyrolytic products, revealed that at a high pyrolysis temperature, proteins and lipids were the predominant contributors to the pyrolytic biocrude phase. Notably, the model predicted the distribution of the solid residue, biocrude, and gaseous products over a wide range of pyrolysis temperatures and holding times. Accordingly, a high pyrolysis temperature resulted in the rapid conversion of microalgae into pyrolytic products. Thus, to obtain a high yield of biocrude, the pyrolysis conditions should be controlled at a high temperature and short time. Meanwhile, a high temperature and long holding time can accelerate the production of gaseous products.

ACKNOWLEDGEMENTS

This work was supported by the Basic Science Research Program (NRF-2019R1A2C1090693) and the Engineering Research Center of Excellence Program (NRF-2021R1A5A6002853) through the National Research Foundation (NRF) funded by the Ministry of Science and ICT, Republic of Korea.

REFERENCES

1. S. Ceylan and D. Kazan, *Bioresour. Technol.*, **187**, 1 (2015).
2. A. F. Ferreira and A. P. Soares Dias, *J. Chem. Technol. Biotechnol.*, **95**, 3270 (2020).
3. C. Yang, R. Li, B. Zhang, Q. Qiu, B. Wang, H. Yang, Y. Ding and C. Wang, *Fuel Process. Technol.*, **186**, 53 (2019).
4. R. Gautam and R. Vinu, *React. Chem. Eng.*, **5**, 1320 (2020).
5. K. Wang and R. C. Brown, *Green Chem.*, **15**, 675 (2013).
6. T. K. Vo, S.-S. Kim, H. V. Ly, E. Y. Lee, C.-G. Lee and J. Kim, *Bioresour. Technol.*, **241**, 610 (2017).
7. T. K. Vo, O. K. Lee, E. Y. Lee, C. H. Kim, J.-W. Seo, J. Kim and S.-S. Kim, *J. Chem. Eng.*, **306**, 763 (2016).
8. P. Supaporn, H. V. Ly, S.-S. Kim and S. H. Yeom, *Environ. Eng. Res.*, **24**, 202 (2019).

9. X. Lu, H. Guo, H. Que, D. Wang, D. Liang, T. He, H. M. Robin, C. Xu, X. Zhang and X. Gu, *J. Anal. Appl. Pyrolysis.*, **154**, 105013 (2021).
10. B. Qu, A. Li, Y. Qu, T. Wang, Y. Zhang, X. Wang, Y. Gao, W. Fu and G. Ji, *J. Anal. Appl. Pyrolysis.*, **152**, 104949 (2020).
11. C. Zhang, Z. Zhang, L. Zhang, H. Zhang, Y. Wang, S. Hu, J. Xiang and X. Hu, *Biomass Bioenergy*, **143**, 105801 (2020).
12. J. Lai, Y. Meng, Y. Yan, E. Lester, T. Wu and C. H. Pang, *Korean J. Chem. Eng.*, **38**, 2235(2021).
13. K. M. Qureshi, A. N. K. Lup, S. Khan, F. Abnisa and W. M. A. W. Daud, *Korean J. Chem. Eng.*, **38**, 1797 (2021).
14. Z. Hu, X. Ma and C. Chen, *Bioresour. Technol.*, **107**, 487 (2012).
15. H. Li, Z. Liu, Y. Zhang, B. Li, H. Lu, N. Duan, M. Liu, Z. Zhu and B. Si, *Bioresour. Technol.*, **154**, 322 (2014).
16. Q.-V. Bach and W.-H. Chen, *Bioresour. Technol.*, **246**, 88 (2017).
17. T. K. Vo, H. V. Ly, O. K. Lee, E. Y. Lee, C. H. Kim, J.-W. Seo, J. Kim and S.-S. Kim, *Energy*, **118**, 369 (2017).
18. A. K. Varma, N. Lal, A. K. Rathore, R. Katiyar, L. S. Thakur, R. Shankar and P. Mondal, *Energy*, **218**, 119404 (2021).
19. X. Guo, J. Cai and X. Yu, *J. Anal. Appl. Pyrolysis.*, **154**, 104997 (2021).
20. R. K. Mishra, Q. Lu and K. Mohanty, *J. Anal. Appl. Pyrolysis.*, **150**, 104887 (2020).
21. J. H. Choi, S.-S. Kim, J. Kim and H. C. Woo, *Energy*, **170**, 239 (2019).
22. H. H. Muigai, B. J. Choudhury, P. Kalita and V. S. Moholkar, *Biomass Bioenergy*, **143**, 105839 (2020).
23. Q.-V. Bach and W.-H. Chen, *Energy Convers. Manag.*, **131**, 109 (2017).
24. Y. Hong, C. Xie, W. Chen, X. Luo, K. Shi and T. Wu, *Renew. Energy*, **145**, 2159 (2020).
25. Z. H. Kim and P. Hanwool, *J. Microbiol. Biotechnol.*, **26**, 1098 (2016).
26. Z. Movasaghi, S. Rehman and D. I. ur Rehman, *Appl. Spectrosc. Rev.*, **43**, 134 (2008).
27. B. E. Eboibi, D. M. Lewis, P. J. Ashman and S. Chinnasamy, *RSC Adv.*, **5**, 20193 (2015).
28. H. V. Ly, S.-S. Kim, J. Kim, J. H. Choi and H. C. Woo, *Energy Convers. Manag.*, **106**, 260 (2015).
29. X. Yang, R. Zhang, J. Fu, S. Geng, J. J. Cheng and Y. Sun, *Bioresour. Technol.*, **163**, 335 (2014).
30. S. K. Maity, *Renew. Sustain. Energy Rev.*, **43**, 1427 (2015).
31. T. K. Vo, J.-S. Cho, S.-S. Kim, J.-H. Ko and J. Kim, *Energy Convers. Manag.*, **153**, 48 (2017).
32. S. Grierson, V. Strezov, G. Ellem, R. McGregor and J. Herbertson, *J. Anal. Appl. Pyrolysis.*, **85**, 118 (2009).
33. T. Aysu, N. A. Abd Rahman and A. Sanna, *Energy*, **103**, 205 (2016).
34. P. Biller and A. B. Ross, *Bioresour. Technol.*, **102**, 215 (2011).
35. P. J. Valdez, V. J. Tocco and P. E. Savage, *Bioresour. Technol.*, **163**, 123 (2014).
36. P. J. Valdez and P. E. Savage, *Algal Res.*, **2**, 416 (2013).